α-Synuclein Stimulates a Dopamine Transporter-dependent Chloride Current and Modulates the Activity of the Transporter*[s]

Jarod Swant[‡], J. Shawn Goodwin[‡], Ashley North[‡], Ahmad Abdul Ali[§], Joyonna Gamble-George[‡], Sanika Chirwa[‡], and Habibeh Khoshbouei[‡][1]

From the [‡]Department of Biomedical Sciences, Meharry Medical College, Nashville, Tennessee 37208 and [§]James Madison University, Harrisonburg, Virginia 22807

Background: Dopamine transporter (DAT) and α-synuclein interact, but the mode and mechanism of α-synuclein regulation of DAT activity are less known.
Results: Elevated intracellular α-synuclein alters DAT-mediated currents and activity that are abrogated by DAT blocker and are absent with heat-inactivated α-synuclein.
Conclusion: DAT/α-synuclein interaction at the cell surface alters the ionic coupling of DAT.
Significance: This interaction modulates dopamine transmission and thus neuronal function.

Dysregulation of dopamine (DA) homeostasis is implicated in neurodegenerative diseases, drug addiction, and neuropsychiatric disorders. The neuronal plasma membrane dopamine transporter (DAT) is essential for the maintenance of DA homeostasis in the brain. α-Synuclein is a 140-amino acid protein that forms a stable complex with DAT and is linked to the pathogenesis of neurodegenerative disease. To elucidate the potential functional consequences of DAT/α-synuclein interaction, we explored α-synuclein modulation of DAT activity in midbrain dopaminergic neurons obtained from TH::RFP mice, immortalized DA neurons, and a heterologous system expressing DAT. We used dual pipette whole cell patch clamp recording to measure the DAT-mediated current before and after dialysis of recombinant α-synuclein into immortalized DA neurons. Our data suggest that intracellular α-synuclein induces a Na^+ independent but Cl^--sensitive inward current in DAT-expressing cells. This current is blocked by DAT blocker GBR12935 and is absent when heat-inactivated α-synuclein is dialyzed into these cells. The functional consequence of this interaction on DAT activity was further examined with real-time monitoring of transport function using a fluorescent substrate of DAT, 4-(4-(dimethylamino)styryl)-*N*-methylpyridinium (ASP^+). Overexpression of α-synuclein in DAT-positive immortalized DA neurons and CHO cells expressing DAT decreased the magnitude and rate of DAT-mediated substrate uptake without a decrease in the initial binding of the substrate at the plasma membrane. Taken together our findings are consistent with the interpretation that DAT/α-synuclein interaction at the cell surface results in a DAT-dependent, Na^+-insensitive, Cl-sensitive inward current with a decrease in substrate uptake, suggesting that DAT/α-synuclein interaction can modulate dopamine transmission and thus neuronal function.

The development of effective therapeutic interventions for neurodegeneration requires a better understanding of the early events that precede neuronal loss. Recent work in various disease models has begun to emphasize the significance of presynaptic dysfunction as an early event that occurs before manifestation of neurological disorders (1–9). Dysregulation of dopaminergic transmission is strongly implicated in the pathogenesis of drug addiction, schizophrenia, and Parkinson disease (10–13). Synaptic dopamine (DA)[2] levels are primarily regulated by the dopamine transporter (DAT) (14), a presynaptic membrane protein that is a member of the Na^+/Cl^--dependent co-transporter gene family (15, 16). By removing extracellular DA and recycling it back into the neuron, DAT plays an essential role in the replenishment of synaptic DA and in terminating DA signaling. An increasing number of proteins have been identified that interact with different domains of the dopamine transporter. These interactions suggest that the synaptic distribution and functional properties of DAT can be regulated via interacting proteins. Most of the known DAT-interacting proteins have been identified using the yeast two-hybrid system (Y2H). The DAT-interacting proteins identified to date using the Y2H system include protein that interacts with C kinase-1 (PICK1) (17), the focal adhesion protein Hic-5 (18), α-synuclein (19), receptor for activated C kinase-1 (RACK1), syntaxin (20), and CaMKIIα (21, 22). Although the exact stoichiometry of the interaction is not known, using the yeast two-hybrid system, Lee *et al.* (19) demonstrated that the dopamine transporter physically interacts with α-synuclein, a small synaptic protein (23–25) that is linked to Parkinson disease (26). Formation of a stable complex between α-synuclein and DAT has been further confirmed by co-immunoprecipitation experiments (27, 28) and also verified in the present study.

Abnormal accumulation of α-synuclein is strongly implicated in Parkinson disease. For example, massive accumulation

[2] The abbreviations used are: DA, dopamine; DAT, dopamine transporter; ASP^+, 4-(4-(dimethylamino)styryl)-*N*-methylpyridinium; CFP, cerulean fluorescent protein.

of α-synuclein in the substantia nigra of patients with triplication of α-synuclein and in midbrain dopamine neurons of chronic cocaine abusers are reported (29–33). Recently, Tong *et al.* (33) reported that high concentrations of α-synuclein (more that 1700% of control) are found in neurodegenerative disorders such as Parkinson disease, familial Parkinsonism with dementia, and multiple system atrophy. Similarly, the Mash laboratory (30) reported overexpression of α-synuclein in dopamine neurons of cocaine abusers. Therefore, the studies reported here focus on the consequence of overexpression of α-synuclein.

Unlike findings for α-synuclein knock-out mice (5), it has been shown that dopamine levels in the brains of null mice for both α- and β-synucleins are decreased by ~20% (5). Mice null for only α-synuclein have a largely normal phenotype (5). In contrast, increased expression of α-synuclein reduces neurotransmitter release by inhibiting vesicle re-clustering and endocytosis (4) as well as inhibition of catecholamine release from adrenal chromaffin cells (34). In dopaminergic-like cell lines, α-synuclein overexpression increases membrane conductance reminiscent of a leak channel (35), suggesting a physiological role for membrane-destined α-synuclein (35).

The role of α-synuclein in dopaminergic transmission and its underlying mechanism is not fully understood, primarily because data to date appear conflicting. Although Lee *et al.* have shown that α-synuclein overexpression results in DAT clustering at the plasma membrane and increased DAT function (19), Wersinger and Sidhu (27, 28) have reported a decreased cell surface expression of DAT and inhibition of DAT activity when α-synuclein is overexpressed.

To address these conflicting findings and further explore the functional consequences of DAT/α-synuclein interaction at the cell surface, we utilized single cell dual pipette whole cell patch clamp recordings to measure DAT-mediated current before and after dialysis of recombinant α-synuclein into immortalized DA neurons expressing dopamine transporter. We found that introducing α-synuclein intracellularly induces a Na^+-independent but Cl^--sensitive inward current in immortalized DA neurons and DAT-expressing cells, which is eliminated by the DAT antagonist GBR12935 and is absent when the cell is dialyzed with heat-inactivated α-synuclein. Furthermore, our finding suggests that overexpression of α-synuclein decreases DAT-mediated substrate uptake without decreasing the overall number of transporters at the membrane.

EXPERIMENTAL PROCEDURES

Reagents and drugs were purchased from Sigma unless otherwise noted. α-Synuclein was purchased from Millipore (Temecula, CA). α-Synuclein cDNA plasmid was a generous gift from Dr. Ted M. Dawson, Johns Hopkins School of Medicine.

Primary Neuronal Culture of Acutely Dissociated TH::RFP Mouse Midbrain Dopamine Neurons

All animals were treated in accordance with the Guide for the Care and Use of Laboratory Animals. Mouse midbrain neuronal cultures were obtained from a transgenic mouse strain gen-erated as described previously (36). Briefly, the tyrosine hydroxylase promoter-driven red fluorescent protein transgene (TH::RFP) was constructed by ligating a 4.5-kb HindIII/EcoRI fragment of the rat tyrosine hydroxylase promoter with DsRed2–1 (Clontech, Palo Alto, CA). The acutely dissociated mouse midbrain dopaminergic neurons from 1–3-day-old pups were isolated and grown on a monolayer of glial cells on poly-D-lysine-treated glass-bottom dishes as we have described previously (21, 37). These neurons were used for the electrophysiology recordings according to our previous reports (21, 37).

Immortalized DA Neuronal Culture, Cell Lines, and Cell Culture

The immortalized DA neurons 1RB3AN27 cells or 1RB3AN27 cells overexpressing human DAT used in this study were gifts from Dr. Haley Melikian (University of Massachusetts) and have been characterized previously (38–43). The immortalized DA neurons were originally derived from fetal rat mesencephalon and were characterized and tested in 6-hydroxydopamine-lesioned rats by Freed and co-workers (38). Cells double every 26 h, which upon differentiation contain tyrosine hydroxylase and DAT proteins and their respective mRNAs. If untreated, the undifferentiated neurons only have the potential to express DAT. For electrophysiology experiments we used undifferentiated immortalized DA neurons (1RB3AN27 cells) and undifferentiated immortalized DA neurons overexpressing human DAT. Immunocytochemistry experiments have confirmed previous reports that undifferentiated immortalized DA neurons do not express DAT unless they are engineered to overexpress DAT (data not shown). Cells were grown in RPMI medium supplemented with 5% glutamine, 10% fetal bovine serum at 37 °C, and 5% CO_2. To keep the DAT-expressing cells under selection, 1 μl/ml G14 was added to the media. For imaging experiments, where we needed a fluorophore-transporter fusion protein to track the transporter in real time, we used parental or stably over expressing YFP-DAT CHO cell lines. The CHO cell lines were gifts from Dr. Jonathan Javitch (Colombia University). Previous studies have shown that these cells are flat, have minimal basal fluorescence, and are suitable for image analysis (39). The cells were grown in F12 medium supplemented with 10% fetal bovine serum, 5% glutamine at 37 °C and 5% CO_2, and 1.5 μl/ml hygromycin.

Subcloning of α-Synuclein into Enhanced Cerulean Fluorescent Protein (CFP) Expression Vector

The cDNA encoding α-synuclein was subcloned into enhanced CFP expression vector (a generous gift from Dr. David Piston, Vanderbilt University), using PCR and GGTGAACTTTCATGGATGTATTCATGAAAGGA (upstream) and GCGT CTAGAGGCTTCAGGTTCGTAGTC (downstream). The PCR product was digested with HindIII and XbaI and ligated into multiple cloning sites of pRC/CMV vector. The ligation product was transformed into *Escherichia coli* strain DH5α, and the cDNA was purified and successfully subcloned. cDNA was purified in large scale using Maxi-prep kit (Qiagen, Valencia, CA). Sequencing confirmed the product obtained was α-synuclein.

Western Blot Analysis

Western blot analyses were performed as described previously (21, 33). In brief, YFP-DAT-CHO cells, IRBN27-DAT cells, or midbrain samples were washed with ice-cold 0.1 M PBS, homogenized in lysis buffer (0.01 M Tris-HCl, pH 7.6, 0.1 M NaCl, 0.001 M EDTA, 100 μg/ml PMSF, and 1 μg/ml aprotinin), and then centrifuged at 15000 $\times$ g for 30 min. Protein concentrations were determined using the Bio-Rad D Protein assay (Bio-Rad). 20 μg of total protein was electrophoresed on 10% SDS-polyacrylamide gels and then transferred to Hybond-P™ membranes (GE Healthcare) as described previously (21, 33). The membranes were blocked and then incubated with a primary antibody directed against α-synuclein (1:1000) (Millipore, Billerica, MA) at 4 °C overnight. Immune complexes were detected with an HRP-labeled secondary antibody and ECL+ chemiluminescence reagents (GE Healthcare). To confirm equal protein loading, blots were stripped and reprobed with an anti-α-actin antibody (1:3000; Sigma) for 2 h at room temperature. Signal intensity was measured using densitometric analysis and quantified.

Measurement of DAT-mediated Whole Cell Currents

Cells were plated at 10^5/35-mm culture dish. Attached cells were washed three times with external solution at room temperature. The external solution contained 130 mM NaCl, 10 mM HEPES, 34 mM dextrose, 1.5 mM CaCl$_2$, 0.5 mM MgSO$_4$, and 1.3 mM KH$_2$PO$_4$ adjusted to pH 7.35 with a final osmolarity of 290 mosM. The pipette solution for the whole cell recording contained physiological-like internal solution containing 120 mM CsCl, 0.1 mM CaCl$_2$, 2 mM MgCl$_2$, 1.1 mM EGTA, 10 mM Hepes, and 30 mM dextrose. The dialysis solution contained physiological-like internal solution $\pm$5 μM α-synuclein or heat-inactivated α-synuclein (as specified in the "Materials and Methods" and "Results" sections). In ion substitution strategies we used either iso-osmotic substitution of choline for Na$^+$ in the external solution to completely remove extracellular Na$^+$ or we used partial substitution of extracellular chloride for sodium acetate to increase Cl$^-$ gradient from 133 to 90 mM (*i.e.* extracellular Cl$^-$ concentration decreased to 90 mM). Thus, in all of the experiments, the intracellular Cl$^-$ concentration is at constant levels of Cl$^-$ = 124.2 mM. pH and osmolarity of the internal solutions were kept constant at 7.35 and 270 mosM, respectively.

Patch electrodes were pulled from quartz pipettes on a P-2000 puller (Sutter Instruments, Novato, CA) and filled with the pipette solution. Whole cell currents were recorded using an Axopatch 200B (Molecular Devices, Sunnyvale, CA) with a low-pass Bessel filter set at 1000 Hz. Current-voltage relations were generated using a voltage step (500 ms) protocol ranging from -100 to $+60$ mV separated by 20 mV from a holding potential of -20 mV. Data were recorded and analyzed off-line using pCLAMP9 software (Molecular Devices).

We used a technique we term "dual whole cell patch clamp" electrophysiology, a modification of a recording configuration used by Mazzanti and DeFelice (44, 45) to determine the effect of α-synuclein on DAT-mediated whole cell currents in immortalized DA neurons stably overexpressing DAT. The dual whole cell patch clamp electrophysiology was performed as follows; one electrode is designated as the recording electrode, and the second electrode is designated as the dialysis electrode. 1) Two gigaohm seals are acquired with two electrodes on the same cell. 2) Whole cell voltage clamp mode is achieved in the "recording" electrode, and 10 min later an I(V) curve is measured. 3) Whole cell current clamp is achieved in the "dialysis" electrode. We briefly placed the recording electrode in current clamp mode, whereas the membrane test voltage verified break-in of the dialysis electrode. Once the dialysis electrode has achieved whole cell configuration, it is placed in current clamp mode, and the recording electrode is returned to voltage clamp mode. Our laboratory and other laboratories have demonstrated that maximum dialysis occurs within 8–10 min after establishing the whole cell configuration (46–48). The cell is thereby dialyzed with the contents of the dialysis electrode for 10 min followed by an I(V) recording (Fig. 1) (using command potentials generated by the voltage clamp recording electrode). As a control, the voltage of the dialysis electrode was monitored to assure the recording electrode had a tight voltage clamp throughout the experiment. The dual whole cell technique was performed with the recording and dialysis electrodes both containing internal solution (37, 46–48), as described (Fig. 1), or the recording electrode filled with internal solution and the dialysis electrode containing internal solution +5 μM α-synuclein or heat-inactivated α-synuclein (Fig. 2). The dual whole cell experimental configuration permits measurement of I(V) before and after α-synuclein dialysis. The external solution contained either external solution or contained an iso-osmotic ion substitution when ion substitution strategies were conducted. In this document consistent with electrophysiological nomenclature, an "inward" current refers to an ionic event that requires the clamp electrode to pass negative current into the cell to keep the voltage clamped at a given potential. As such, the term inward in this context does not refer to the direction of the ion flow; hence, the flow of positive ions into the cell and/or flow of negative ions out of the cell both produce an inward current. In this study the DAT-dependent current is defined as currents we measure, based on our previous studies (46–48), that are blocked by DAT blockers, like GBR12935.

Selection of the 5 μM Concentration of α-Synuclein for Use in Our Recording Pipette

We used quantitative or semiquantitative neurochemical measurements of the full-length 19-kDa α-synuclein that was extrapolated against a standard curve calibrated by using 1) purified recombinant α-synuclein, 2) cells overexpressing α-synuclein, and 3) α-synuclein levels in the midbrain region of animals treated with neurotoxic doses of methamphetamine (an animal model of system atrophy).[3] These criteria suggest that 5 μM recombinant α-synuclein (approximately 0.07 μg of recombinant human α-synuclein) can be detected as a 19-kDa protein (supplemental Fig. 2) and is in the median range of our quantitative or semiquantitative neurochemical measurements. Therefore, in a reduced system such as ours, 5 μM α-sy-

---

[3] J. Gamble-George and H. Khoshbouei, unpublished data.

nuclein in the recording pipette may actually be an underestimation of actual increase in α-synuclein levels reported in synucleinopathies (see the Introduction), (29–33).

Measurement of DAT Activity Using ASP⁺, a Fluorescent Substrate of DAT

The experiments were performed as previously described (49–53). For ASP^+ experiments, cells were plated at 10^5/ 35-mm glass-bottom MatTek Petri dish (MatTek, Ashland, MA). CHO or immortalized DA neurons cells stably expressing YFP-DAT were transiently transfected with CFP-α-synuclein. The DAT-mediated ASP^+ uptake was similar in either cell lines. Images of CHO-YFP-DAT cells are shown because these cells provide better visualization of the data. The addition of YFP tag to DAT does not alter transporter-mediated activity (37, 47, 48, 54, 55). The cells were washed 2× with external solution with a final pH of 7.35 and osmolarity of 290 mosm as described above. 1 ml of external solution was added to the dish, and cells were selected for imaging with a Nikon inverted TE2000-U C1 laser scanning confocal microscope (Nikon, Melville, NY). A 40 × 1.3 NA Plan-fluor objective (Nikon) was used with the confocal pinhole set to one Airy unit. Pilot experiments at both room temperature and 37 °C were performed; the relative difference between experimental conditions was unchanged regardless of temperature (data not shown); however, to be comparable with the preponderance of the ASP^+ literature (51–53, 56, 57) and electrophysiology data in this study as well as others (21, 37, 58–63), we chose to perform our experiments at room temperature. The cells were selected with the appropriate filter sets. The CFP-α-synuclein was identified using a CFP-specific filter set, and YFP-DAT was identified using a YFP filter set. For analysis purposes, at the start of each experiment 512 × 512 pixel reference images showing cells expressing YFP-DAT alone, cells co-expressing CFP-α-synuclein/YFP-DAT, cell expressing CFP-α-synuclein alone, or cells expressing neither protein were saved and labeled for analysis. This provides an internal experimental control because not every cell co-expresses both proteins. Using this approach, real time quantification of DAT-mediated substrate uptake in single cells was measured using the high affinity, fluorescent DAT substrate ASP^+ (51, 56, 57). The sampling frequency was 1.52 frame per second (fps) over 8 min that provided 692 images. After 10 base-line images, ASP^+ was added to a final concentration as noted under "Results" (Figs. 5 and 6). ASP^+ was excited at 488 nm and detected at 590/50 nm. The emission of YFP signal is significantly blue-shifted compared with ASP^+ maximum emission that minimizes bleed-through into the ASP^+ channel. At the start of each experiment, the detector gain in the ASP^+ channel was adjusted to offset any base-line YFP bleed-through (52, 53, 55).

ASP⁺ Uptake Analysis

Data were pooled from at least three separate transfections, with a minimum of four independent experiments per transfection. Cell boundaries were determined from an image showing both YFP intensity and differential interference contrast images saved before the timed experiment. Binding and transport of ASP^+ was determined from the average fluorescent units of

each individual cell throughout each experiment using the NIS elements software package (Nikon). Within each experiment three groups of cells were selected for analysis: YFP-DAT/CFP-α-synuclein, YFP-DAT/only, and cells expressing neither protein. This approach provided an internal control resulting in the evaluation of the two experimental groups under identical conditions. Fluorescence measurements were normalized by dividing the average of the first four fluorescence values. Values are shown as the fold change in ASP^+ fluorescence, and the rate was defined as the slope of ASP^+ uptake (53, 55) (from a linear fit line from the data at $t = 75$–250 s).

Choice of Cells for Various Experiments

For electrophysiological studies we used immortalized DA neurons, *i.e.* 1RB3AN27 cells overexpressing human DAT. The results were confirmed in CHO-YFP-DAT cells and midbrain DA neurons obtained from primary neuronal culture of acutely dissociated TH::RFP mouse midbrain dopamine neurons. For control experiments we used relevant parental cells not expressing DAT.

For DAT-mediated substrate (ASP^+) uptake studies, we used immortalized DA 1RB3AN27 neuronal cells overexpressing DAT. All of the uptake experiments were confirmed in CHO-YFP-DAT cells. We have shown images of CHO-DAT cells because these cells have low background fluorescence and thus less confounding visual representations of the data. We were not able to use primary cultures from midbrain DA neurons of TH::RFP mouse for the uptake experiments because the high endogenous fluorescence of these cells confounded detection of ASP^+.

Statistical Analyses Performed

Electrophysiology Experiments—Data are shown as the mean ± S.E. Unless otherwise noted, analysis of variance with post hoc Newman-Keuls was used for the statistical comparison of more than two means. The two-tailed, unpaired Student's *t* test was applied when two means were compared.

ASP⁺ Experiments—Data are shown as the mean ± S.E. unless otherwise noted. In ASP^+ competition experiments, the data were fit with GraphPad Software Prism 5.0 using the least squares method to fit a regression line (at $t = 75$–250 s). (Fig. 6A). Data were analyzed for rejection of the null hypothesis using a one-way analysis of variance followed by a Bonferroni post hoc test (Figs. 5 and 6; supplemental Tables 1 and 2). Tests were performed using Prism Version 5.0 statistical software package (GraphPad Software). A value of $p < 0.05$ was considered statistically significant. F values, degrees of freedom, and significance are also documented in supplemental Tables 1 and 2.

RESULTS

Dual Patch Clamp Recording Does Not Affect DAT-mediated Whole Cell Currents and DAT Reversal Potential—Formation of a stable complex between α-synuclein and DAT has been further confirmed by co-immunoprecipitation experiments (27, 28) and also verified in the present study (supplemental Fig. 1). To determine the regulatory role of α-synuclein on DAT-mediated whole cell currents in immortalized DA neurons sta-

bly overexpressing DAT, we used dual patch clamp electrophysiology (44, 45). Conventional whole cell patch clamp can measure DAT-related activity by using a single patch electrode for both dialysis of internal solution and recording, a technique that has been used successfully by us and other groups (37, 46, 48). In this study, to effectively determine the regulatory role of α-synuclein on the electrogenic properties of DAT, we used a dual patch clamp recording technique that provides measurement of DAT-mediated currents in the presence or absence of intracellular α-synuclein in the same cell. We measured DAT-mediated currents when physiological-like internal solution, α-synuclein, or heat-inactivated α-synuclein were dialyzed into the cell as described under "Experimental Procedures." The current-voltage I(V) relationships, when both recording and dialysis electrodes filled with physiological-like solution, were examined when the membrane potential was stepped from +60 mV to −100 mV in 20-mV increments, generated after single and double whole cell configurations (Fig. 1). These current-voltage I(V) relationships were virtually overlapping (Fig. 1). The amplitude of DAT-mediated currents at −100 and the reversal potentials measured under these conditions were, respectively, −22.2 ± 7.27 pA (single) and −19.3 ± 6.9 pA (double) for the whole cells currents and −35.4 ± 2.1 mV (single) and −33.73 ± 1.8 mV (double) for the reversal potential, ($n = 7$). These values are little changed from single to double whole cell configuration and are consistent with reported DAT-mediated currents in the literature (37, 46, 48, 62, 63). These findings suggest that our dual patch clamp recording strategy is a viable approach for determining whether α-synuclein regulates DAT-mediated currents.

α-Synuclein Increases DAT-mediated Inward Currents and Induces a Rightward Shift in the DAT-mediated Current-Voltage I(V) Relationship—DAT-mediated currents are ion- and voltage-dependent (58, 59, 62, 63), and that can potentially affect the membrane microenvironment near the transporter and the activity of other targets (61, 62). To determine whether α-synuclein regulates DAT-mediated currents, we introduced 5 μM recombinant α-synuclein or 5 μM heat inactivated α-synuclein (Fig. 2) into the dialysis electrode. Dialysis of α-synuclein into the cell increased the inward currents at membrane potentials close to and below the resting membrane potential but had minimal effect on the electrogenic properties of DAT at potentials above −20 mV. Compared with the absence of α-synuclein, the intracellular α-synuclein increased the magnitude of currents at −80 and −100 mV about 3.9- and 3.3-fold, respectively, when the I(V) plot is normalized (Fig. 2 and supplemental Fig. 3, showing the normalized I(V) plot). In contrast, intracellular α-synuclein had minimal effect on DAT-mediated currents at potentials above −20 mV. Overall, α-synuclein-stimulated currents produced a net depolarizing effect on the DAT reversal potential, causing an ∼20.6-mV rightward shift (from −33.7 ± 2.7 mV to −17.6 ± 3.07 mV) in the reversal potential (Fig. 2A). Using the Goldman-Hodgkin-Katz equation, when $R = 8.314$ J·K^{-1}·mol^{-1}, $T = 298.15$ K, $F = 96,485$ coulombs·mol^{-1}, $pK = 1$, $pNa = 0.05$, $pCl = 0.45$, $[K]_o = 1.3$ mM, $[K]_i = 0$ mM, $[Na]_o = 130$ mM, $[Na]i = 0$, $[Cl]_o = 133$ mM, $[Cl]_i = 124.2$ mM, the calculated equilibrium potential for chloride is −1.78 mV, which is positive to −17 mV and supports the
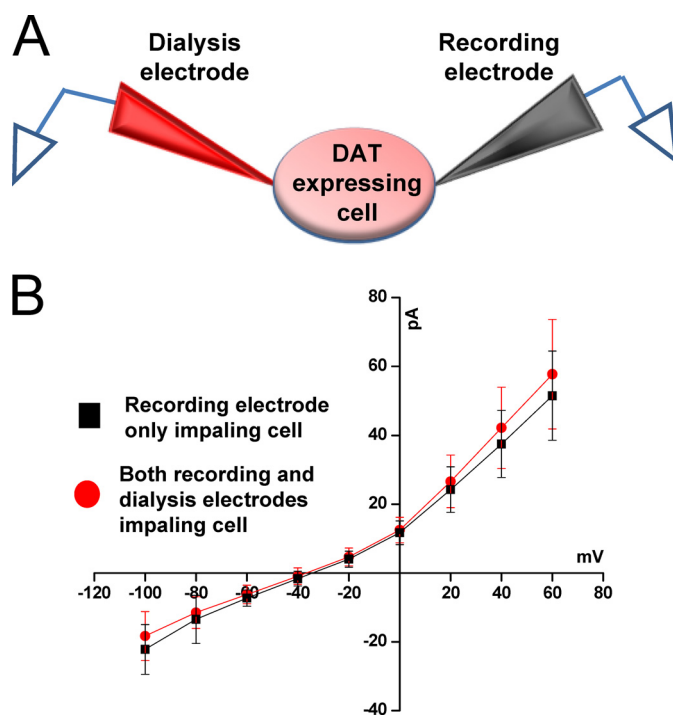

FIGURE 1. **Dual patch clamp technique is an advantageous approach to measure changes in DAT-mediated whole cell currents.** *A*, shown is a schematic presentation of an experimental configuration. Immortalized DA neurons (1RB3AN27 cells) stably overexpressing DAT were voltage-clamped with two patch electrodes (one in voltage clamp mode, the other in current clamp mode). *B*, representative DAT-mediated whole cell currents after single and dual patch clamp show that dual patch clamp does not affect DAT-mediated currents. After obtaining two tight seals, the recording electrode was switched into whole cell voltage clamp configuration, whereas the dialysis electrode was kept in current-clamp mode. After a 10-min equilibration period, whole cell currents were recorded by stepping the membrane potential in 20-mV steps (+60 to −100 mV), from a holding potential of −20 mV. The dialysis electrode was then gently transitioned into the whole cell configuration and quickly switched back to current clamp mode. This electrode remained in current clamp mode throughout the rest of the experiment. Ten minutes after the dialysis electrode assumed whole cell configuration, a second I(V) was generated. Both electrodes contained physiological-like internal solution (see above) ($n = 7$).

idea that this may be a Cl$^-$ current. Changes in inward currents mediated by α-synuclein are blocked by the DAT antagonist GBR 12935 (5 μM), indicating that these currents are DAT activity-dependent (Fig. 2C).

In parallel experiments we found that overexpression of α-synuclein depolarizes DAT cells and that this depolarized state of the cell is a consequence of α-synuclein expression. As shown in Fig. 2B, the resting membrane potential in DAT/α-synuclein-expressing cells was −20.3 ± 3.2 mV compared with DAT only cells −36.5 ± 5.5 mV ($p < 0.05$).

Dialysis of heat-inactivated α-synuclein (5 μM, 10 min 70 °C) did not affect the magnitude of the inward currents or the reversal potential (Fig. 2D). Therefore, it appears that intracellular α-synuclein might have a direct or indirect effect on ionic permeability of DAT-associated inward current.

The dialysis of α-synuclein (5 μM) via the recording electrode into the DA neuron obtained from the acutely dissociated midbrain region of TH::RFP mice also produces an increase in inward currents at −60, −80, and −100 mV membrane potentials (Fig. 3). Therefore, our result is consistent with the interpretation that the impact of α-synuclein overexpression on

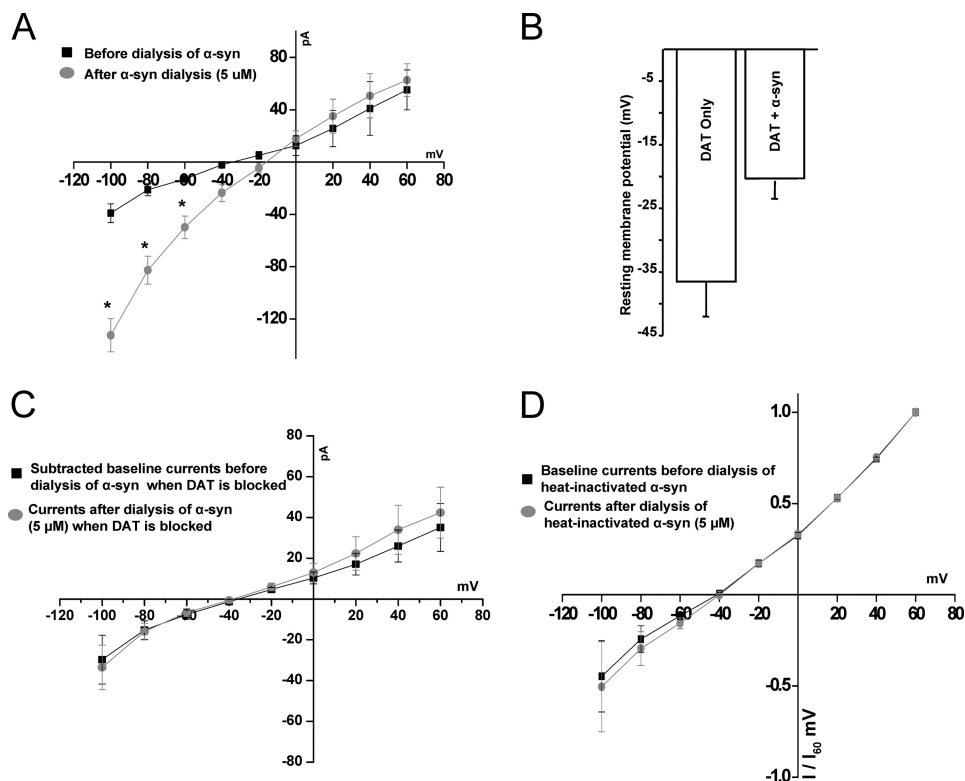FIGURE 2. *A* and *B*, α-synuclein increases DAT-mediated inward currents and induces a rightward shift in the current-voltage I(V) relationship. *A*, the experiments were performed as in Fig. 1 except the dialysis electrode contained 5 μM α-synuclein. Briefly, after two tight seals were obtained, the recording electrode was transitioned into whole cell configuration. The whole cell currents were recorded as described in Fig. 1. The dialysis electrode containing 5 μM α-synuclein was then switched to whole cell configuration, dialyzing the recombinant α-synuclein into the cell for 10 min. Whole cell currents were recorded at this time ($n = 4–5$). *B*, shown are resting membrane potentials of cells expressing DAT only or DAT with and without α-synuclein ($n = 6$). *C*, active dopamine transporter is required for α-synuclein-stimulated increase in inward currents. A 5-min pre-application of a DAT blocker, GBR 12935 (5 μM), eliminates the effect of α-synuclein on inward currents and the rightward shift in the current voltage relationship. The *black squares* represent GBR12935 subtracted base-line currents. The *circles* represent the currents after the dialysis of α-synuclein into the cell when the transporter is blocked ($n = 4$) *D*, heat-inactivated α-synuclein does not increase the inward currents or affect the reversal potential. Averaged normalized whole cell currents before and after dialysis of heat-inactivated α-synuclein into the cell are shown; experiments were performed as in Figs. 2 and 3. Whole cell currents were recorded before and 10 min after dialysis of heat-inactivated α-synuclein into the cell. There is no effect on the reversal potential of the I(V) curve with intracellular heat-inactivated α-synuclein ($n = 4$).

DAT activity (*i.e.* DAT-mediated DA uptake (see below)) is independent of cellular background, such that α-synuclein overexpression increases DAT-mediated inward currents and decreases DAT-mediated DA uptake in cell types studied.

Endogenous Physiological Levels of α-Synuclein Have No Detectable Effect on DAT-mediated Currents—α-Synuclein expression in mouse midbrain, 1RB3AN27-DAT, and YFP-DAT-CHO cells was examined by Western immunoblot analysis as described under "Experimental Procedures" and compared with dilution standards of recombinant α-synuclein (supplemental Fig. 2, *A–C*). The Western blot analysis suggests that, unlike native midbrain neurons, the undifferentiated 1RB3AN27-DAT and YFP-DAT-CHO cells do not express α-synuclein (supplemental Fig. 2C). It is also possible that the expression level of α-synuclein in these cells is below our detection limit.

To test whether endogenous physiological levels of α-synuclein influence the dopamine transporter-induced inward currents, we determined DAT-mediated inward current in whole cell configuration in DA neurons (which express endogenous physiological levels of α-synuclein) compared with undifferentiated 1RB3AN27-DAT and YFP-DAT-CHO cells (which lack α-synuclein). Consistent with the previous reports, we found no significant difference in DAT-mediated inward

currents in DA neurons and DAT-expressing heterologous cells lacking endogenous α-synuclein expression (supplemental Fig. 2, *C* and *D*) (37, 47, 48). Taken together our findings are consistent with the interpretation that the endogenous levels of α-synuclein may not influence the activity of DAT in a measurable level, but it is the overexpression of α-synuclein that alters the activity of dopamine transporter.

α-Synuclein-stimulated Inward Currents Do Not Require Extracellular Na^+ Ions—Currents identified for DAT are Na^+/Cl^--dependent, and they include 1) a transport current reflecting substrate movement and 2) an uncoupled current that can be blocked by DAT inhibitors. Inward currents in voltage clamp mode are mediated by positive ions entering the cell and/or negative ions leaving the cell. Because intracellular α-synuclein-modulated an inward current in the absence of substrate, we hypothesized that α-synuclein-modulated currents are caused either by an increase in inward movement of Na^+ or outward movement of Cl^-. We used ion substitution strategies to examine this hypothesis. With the iso-osmotic substitution of choline chloride for NaCl in the external solution in the presence of intracellular α-synuclein (5 μM), the inward currents were still 3–4-fold larger than the currents measured in the absence of α-synuclein (4.2 ± 1.4 at -100 mV) ($n = 4$; Fig. 4A). Consistent with previous reports by Ingram *et al.* (61, 62) and
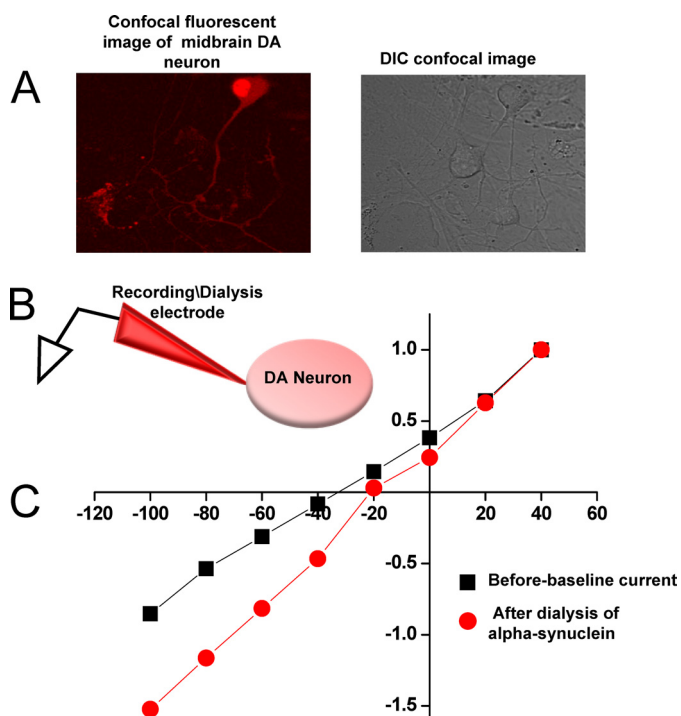
FIGURE 3. *A–C, dialysis of α-synuclein into DA neuron increases DAT-mediated inward currents and induces a rightward shift in the current-voltage I(V) relationship.* *A,* the *left panel* depicts a confocal fluorescent image of midbrain DA, and the *right panel* is the differential interference contrast (*DIC*) confocal image of the same field showing that in the acutely dissociated midbrain primary culture a DA neuron can be selected for recording. Panel *B* depicts the experimental configuration of α-synuclein dialysis into the neuron via the recording electrode. *C,* the voltage-current relationship at time 0 (*black squares*) and 10 min after dialysis of α-synuclein (*red circles*) into the neuron is shown.

Sonders *et al.* (63), because Na^+ carries some of the DAT-mediated current, we measured a smaller inward current in the absence of extracellular Na^+ (61–63) ($n = 4$; Fig. 4*A*). Furthermore, in the absence of extracellular Na^+, α-synuclein still sustained the rightward shift in the reversal potential (-46.5 ± 5.5 mV of DAT cells before dialysis of α-synuclein *versus* -19.2 ± 8.3 mV of DAT cell after dialysis of α-synuclein ($p < 0.05$)) (Fig. 4*A*). These findings confirm that even in the absence of extracellular Na^+ ions, α-synuclein still increases a DAT-mediated inward current and induces a rightward shift in the DAT-mediated current-voltage I(V) relationship.

α-Synuclein-mediated Inward Current Is Sensitive to Cl^- Gradient—DAT-activated conductance is mainly due to transport of Cl^- ions through the transporter (58, 61, 62). To examine the Cl^- dependence of α-synuclein-modulated currents via DAT, we used ion substitution to increase the Cl^- gradient across the plasma membrane by ~30%. Iso-osmotic substitution of extracellular NaCl with sodium acetate (extracellular Cl^- concentration decreased from 133 to 90 mM, and internal Cl^- kept constant at 124.2 mM, pH 7.35) provides a Cl^- gradient where inside Cl^- is greater than outside Cl^-. The calculated ECL in this condition is ~+8 mV. Under these conditions there is an additional increase in α-synuclein-modulated inward currents compared with control solutions (Fig. 4*B*, $n = 5$). These findings suggest that α-synuclein may directly or indirectly affect the transport-associated currents by increasing outward Cl^- transport.

α-Synuclein Decreases DAT-mediated Substrate Uptake— To determine the consequences of α-synuclein/DAT interaction on the activity of DAT, we used a fluorescent tool, ASP^+, (49–53) that allows quantitative measurement of substrate uptake into DAT-expressing cells, with millisecond time resolution at the single cell level in the presence and absence of intracellular α-synuclein. Consistent with previous reports, we found that ASP^+ rapidly binds at the membrane and is transported into DAT-expressing cells (49–53). Fluorescent DAT substrate ASP^+ was added to cells that expressed either YFP-DAT (Fig. 5*A*, *left panel*) or YFP-DAT and CFP-α-synuclein (Fig. 5*A*, *middle panel, merge right panel*). The ASP^+ uptake was quantified as changes in fluorescence levels in the cytoplasm of DAT-expressing cells with and without α-synuclein compared with base-line measure. The background signal is defined as nonspecific fluorescence levels of cells not expressing YFP-DAT and is subtracted. The DAT-mediated ASP^+ binding and transport were characterized by a rapid (in milliseconds) binding phase, where ASP^+ fluorescence accumulated at the cell membrane, and an uptake phase, where ASP^+ signal increased in the cell cytoplasm (Fig. 5*B*). The accumulation of ASP^+ into the DAT-expressing cells increased linearly in a time-dependent fashion. The rate of ASP^+ uptake was quantified by linear regression of the data between 75 and 250 s, fit by least squares regression to a straight line between those time points (minimum $r^2 > 0.95$). Compared with DAT cells, the cells that expressed both α-synuclein and DAT had a decreased rate of ASP^+ uptake (Fig. 5, *C* and *D*, and supplemental Table 1). As predicted, increasing ASP^+ concentrations increased the magnitude of ASP^+ uptake in both DAT and DAT/α-synuclein cells; nonetheless, the rate of ASP^+ uptake was lower in DAT/α-synuclein cells. The total DAT protein levels (supplemental Fig. 1) and the maximum initial ASP^+ binding was not different between the two groups (Fig. 5*C*).

In the competition experiments extracellular DA decreased the uptake of ASP^+ in a concentration-dependent fashion (Fig. 6*B*), confirming that DA and ASP^+ uptake occur via similar pathway. The presence of α-synuclein in cells in these experiments also resulted in decreased ASP^+ uptake (Fig. 6, *A* and *B*). The log[DA] *versus* slopes in the competition experiments were nonlinear fit by the least squares method (Fig. 6*B*), with a calculated IC_{50} of 1.2 μM. Intracellular α-synuclein increased the IC_{50} to 2.9 μM (Fig. 6*B*, supplemental Table 2).

Unlike the rate of ASP^+ uptake, the maximum ASP^+ binding at the plasma membrane in YFP-DAT/CFP-α-synuclein cells compared with YFP-DAT/CFP-empty vector cells and YFP-DAT cells were not different. The last two groups have identical uptake rates. In addition, at time 0 before the start of each experiment, the level of YFP fluorescence at the membrane of YFP-DAT/CFP-α-synuclein cells was not lower than the YFP fluorescence levels at the membrane of YFP-DAT/CFP-empty vector cells and YFP-DAT cells. The total DAT protein levels (supplemental Fig. 1) and the maximum ASP^+ binding at time 0 was not different between the groups (Fig. 5*C*). These findings suggest that α-synuclein decreases the uptake rate of the substrate via DAT by decreasing the activity, but not levels of the transporter at the plasma membrane.
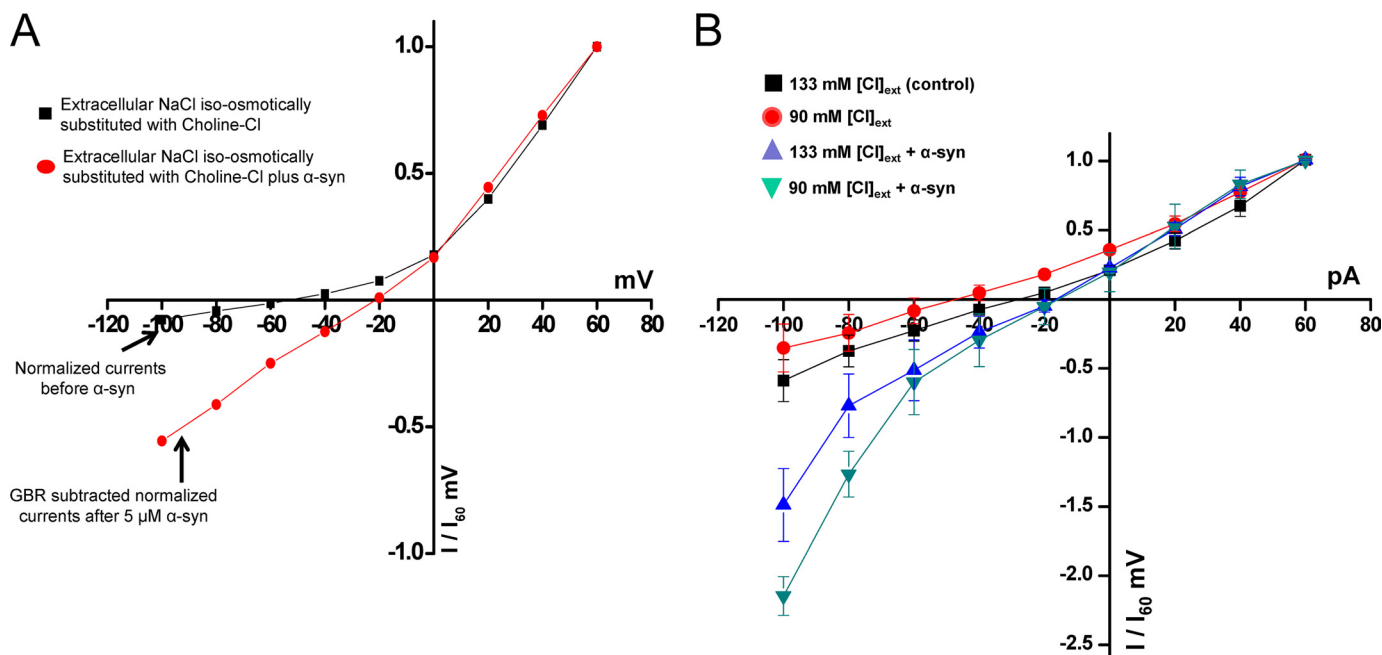
FIGURE 4. *A*, α-synuclein-mediated inward currents are not dependent on extracellular Na^+. The experiments were performed as in Figs. 1 and 2. Representative I(V) for the iso-osmotic substitution of choline chloride for NaCl in the external solution in the absence (*black squares*) or presence (*red circles*) of 5 μM α-synuclein. Note the decrease in DAT-mediated inward current (*black squares*) in the absence of extracellular Na^+ as reported by Sonders *et al.* (63). Intracellular α-synuclein sustains an increase in the GBR12935 sensitive inward currents (*red circles*) in the absence of extracellular Na^+. The intracellular α-synuclein induces a rightward shift in the reversal potential of I(V). The ionic compositions of the solutions in the recording and dialysis electrodes are as described in Fig. 1 and kept constant. The dialysis electrode contained 5 μM recombinant α-synuclein. *Circles* depict GBR12935 sensitive currents (*n* = 4). *B*, the magnitude of α-synuclein-mediated inward current is affected by extracellular Cl^- levels. In the presence of intracellular α-synuclein the GBR 12935-sensitive inward current increases when external Cl^- is reduced (Cl^- gradient is increased). The experiments were performed as described in Figs. 1 and 2 except that the external solution contained either 130 or 90 mM Cl^- (reduced) by iso-osmotic substitution of NaCl with sodium acetate. In all experiments the pH for the intracellular and extracellular solutions was adjusted to 7.35. The osmolarity for internal and external solutions kept constant 270 and 290 mosM, respectively. The dialysis pipette contained α-synuclein or heat-inactivated α-synuclein (*n* = 5).
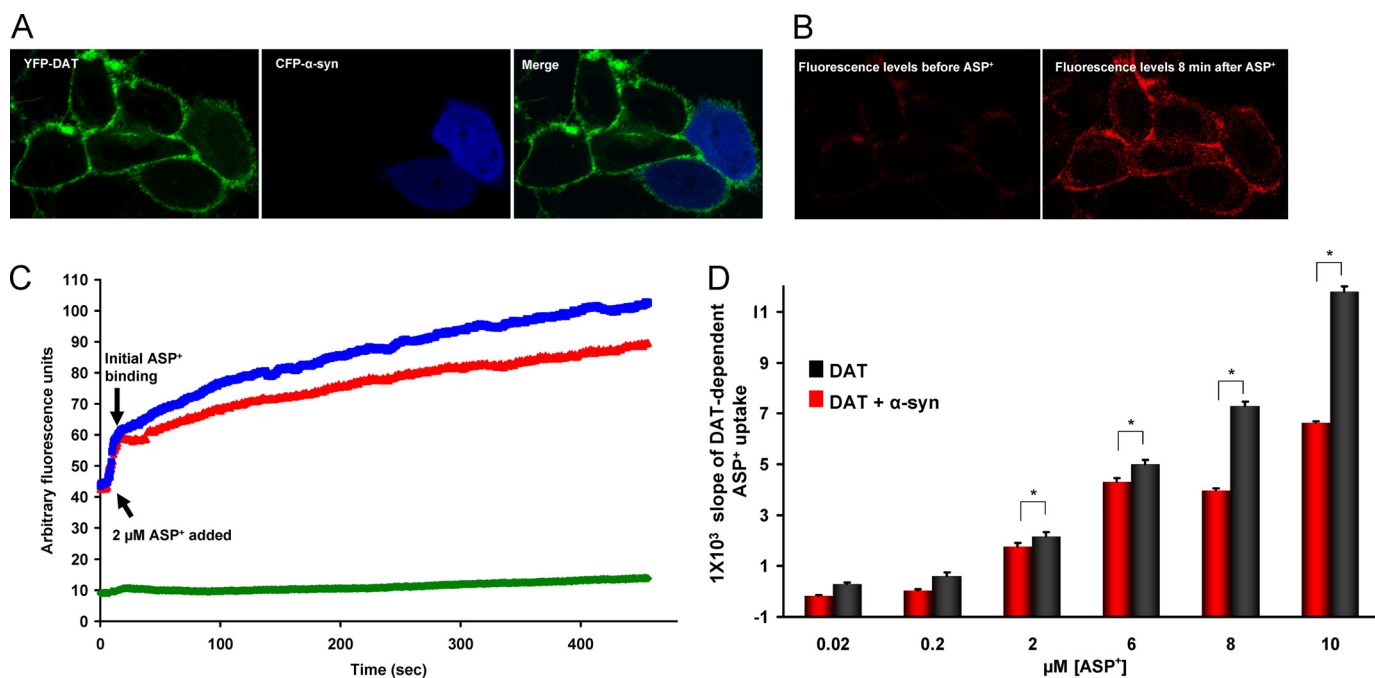

FIGURE 5. *A* and *B*, overexpression of α-synuclein decreases substrate uptake via DAT. *A*, representative images show live cell images of CHO cells stably expressing YFP-DAT, transiently expressing CFP-α-synuclein, and merge. *B*, before and after ASP^+ binding and transport via cell surface DAT is shown. ASP^+ uptake is decreased in α-synuclein expressing cells as measured by a decrease in intracellular ASP^+ fluorescence. *C* and *D*, the rate of DAT-mediated substrate uptake decreases when α-synuclein is overexpressed. *C*, the average uptake rate of 2 μM ASP^+ is decreased when α-synuclein is overexpressed in DAT cells. The *blue line* depicts DAT-expressing cells, the *red line* depicts DAT and α-synuclein-expressing cells, and the *green line* shows cells expressing no dopamine transporter. *D*, shown is a *bar graph* summary of the rate of ASP^+ uptake over multiple concentrations of ASP^+ in DAT cells overexpressing α-synuclein. The *error bars* in *B* depict mean ± S.D., and the values are listed in supplemental Table 1.
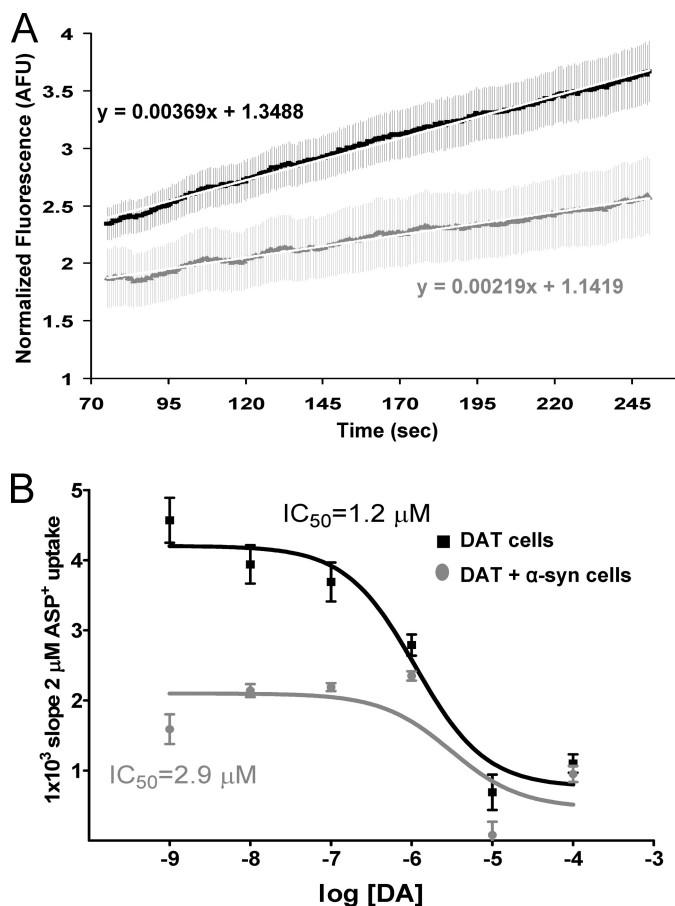
FIGURE 6. α-Synuclein overexpression increases the IC$_{50}$ for DA. *A,* in the presence of dopamine (0.01 μM), the rate of ASP$^+$ uptake is decreased by α-synuclein. *B,* competitive binding curve demonstrates that dopamine competes for ASP$^+$ uptake. Note the lower ASP$^+$ uptake in cells expressing both DAT and α-synuclein. The *error bars* in *B* depict the mean ± S.D., and the values are listed in supplemental Table 2.

DISCUSSION

Regulation of DAT activity plays a key role in extracellular dopamine availability. The findings that DAT interacts with α-synuclein (19, 27, 28), a protein implicated in neurodegenerative disease, provoked our interest in functional consequence of this interaction on DAT activity. High concentrations of α-synuclein (more than 1700% of control level) are found in neurodegenerative disorders such as Parkinson disease, familial Parkinsonism dementia, and multiple system atrophy (33). Using the single cell, dual patch clamp approach, we were able to focus on the impact of α-synuclein on DAT activity in real time. We found that intracellular α-synuclein induces a DAT-mediated inward current that is independent of extracellular Na$^+$ but sensitive to the transmembrane Cl$^-$ gradient. This inward current is eliminated by DAT antagonist GBR12935 and is absent with intracellular heat-inactivated α-synuclein. Intracellular α-synuclein mediates a rightward shift in the DAT reversal potential and depolarizes the membrane. These changes are paralleled by an α-synuclein-dependent decrease in rate of DAT-mediated substrate uptake.

Our studies directly assess the effect of α-synuclein on DAT activity when α-synuclein is dialyzed into DA neuron (21, 37) or immortalized mesencephalic neuronal cells (IRB3AN27) stably

overexpress human dopamine transporter (38, 39, 64) via the patch clamp electrode or when α-synuclein is transiently overexpressed. Dialysis of α-synuclein into the cell via the patch clamp electrode allows real time assessment of DAT activity before and after intracellular α-synuclein under identical conditions and, importantly, in the same cell. Therefore, it provides a unique experimental configuration that can assess the influence of intracellular α-synuclein on the activity of the transporter in a voltage-controlled condition.

DAT-associated currents are reported to arise from the stoichiometric coupling of two Na$^+$ ions transported and one Cl$^-$ ion counter-transported to each molecule of substrate transported (63, 65). However, Sonders *et al.* (63) have shown that DAT-mediated currents can occur in the absence of the substrate and are larger than the predicted stoichiometry of the transport cycle. Therefore, it is postulated that DAT-associated current can be characterized as both coupled and uncoupled currents via both channel and transporter modes of DAT operations (58, 59, 63). Consistent with the literature, we found that dialysis of α-synuclein into the cell via the patch clamp electrode results in a DAT-mediated uncoupled inward current that is eliminated by DAT blocker GBR12935. Intracellular α-synuclein mediates a rightward shift in the DAT reversal potential that may be attributed to increases in the inward flow of Na$^+$ and/or outward flow of Cl$^-$ ions (see below). Consistent with this observation, we found that the membrane potential of DAT cells overexpressing α-synuclein rest at more depolarized membrane potentials (Fig. 2).

We are not the first group to report an increase in the DAT-mediated uncoupled currents (46, 61–63). Similar to the effect of α-synuclein on DAT-associated inward currents in the absence of the substrate, Ingram and Amara (61) previously observed that in the absence of extracellular DA, arachidonic acid (10–100 μM) stimulates a cocaine (DAT blocker)-sensitive, DAT-associated inward current that is 50-fold greater than the inward current normally measured in DAT-expressing oocytes.

We also observe that α-synuclein overexpression depolarizes the membrane potentials from -36.5 ± 5.5 mV in DAT cells and -20.3 ± 3.2 mV in DAT/α-synuclein cells ($p < 0.05$) (Fig. 2*B*). This α-synuclein-regulated change in the resting membrane potential can affect both the excitability of the cell and its energy expenditure. Thus, α-synuclein interaction with DAT may affect neuronal energy consumption that could lead to disruption of cell homeostasis. Because α-synuclein is implicated in neurodegenerative diseases, examination of the metabolic cost of α-synuclein overexpression in dopamine neurons is of interest.

One of our goals in this study was to possibly shed some light on the conflicting data concerning the functional consequences of DAT/α-synuclein interaction. Our data are consistent with previous reports by Wersinger *et al.* (27, 28) that α-synuclein overexpression decreases DA uptake using [^{3}H]DA uptake into cell populations expressing with and without α-synuclein. We do not know why Lee *et al.* (19), also examining [^{3}H]DA uptake in cell populations, see increases in DA when α-synuclein is overexpressed. However, in neither of these [^{3}H]DA uptake studies was it possible to visualize DAT at the cell surface or

measure live cell instantaneous (millisecond) rates of substrate at the single cell level. It is possible that the impact of α-synuclein on DAT-mediated DA efflux, DAT trafficking, or other events that are asynchronous in their multicell studies limit the interpretation of steady state measurement of [³H]DA uptake in the cell population studies.

The magnitude and rate of dopamine uptake and dopamine efflux is determined not only by the number of transporters at the surface membrane but also by the conformational state of the transporters; that is, inward facing conformation *versus* outward facing conformation. These conformational states can be regulated by membrane potential (48), intracellular ions (48, 60, 63), the phosphorylation state of the transporter (47), and membrane cholesterol levels (66). Because we found that total DAT protein (supplemental Fig. 1) and the maximum initial ASP^+ binding between the two groups, DAT cells and DAT with and without α-synuclein cells, were similar (Fig. 5*C*), our data provide yet another level of molecular detail for the impact of α-synuclein on DAT function and are consistent with the interpretation that α-synuclein alters the ionic coupling of DAT to decrease DAT-mediated substrate uptake without any change in the surface expression of DAT.

The dopamine transporter has been shown to affect membrane excitability (62) by inducing an inward Na^+ and Cl^- current (48, 62, 63). The α-synuclein-mediated increase in DAT-mediated inward currents can be a consequence of the direct interactions between these two proteins or secondary to formation of conductive pores (67), a result of pathological levels of α-synuclein inside the neuron. These membrane pores can influence membrane conductance (35, 68), which in turn can impact DAT properties. The data presented in this study cannot exclude these possibilities. However, the studies do affirm the importance of DAT in the changes in currents observed when α-synuclein is overexpressed, as these currents are not detected in the absence of DAT, when the transporter is blocked by an antagonist, or when heat inactivated rather than when native α-synuclein is introduced into the recording pipette.

The variety of ways in which α-synuclein expressed at normal endogenous levels regulates DAT activities is still being clarified. For example, α-synuclein may function as a co-chaperone, as transgenic expression of α-synuclein abolishes the lethality and neurodegeneration caused by deletion of the synaptic vesicle chaperone, cysteine-string protein-α (5, 69). In addition, α-synuclein also has been suggested to be involved in intracellular trafficking, as overexpression of α-synuclein in *Drosophila* and yeast disrupts cargo trafficking within the endoplasmic reticulum (70, 71). Interestingly, mice null for α-synuclein show no immediate phenotype (5), although studies in the context of various stressors in these mice have yet to be performed. Nonetheless, the distinctive neuropathology found in hereditary parkinsonism and dementia is linked to α-synuclein overexpression (72). Thus, our studies are important in revealing the molecular consequences of this increased α-synuclein expression.

Overall, however, our findings provide evidence that interaction of α-synuclein and surface DAT regulates the activity of the transporter that can modulate the synaptic availability of DA in addition to dramatically affecting the membrane microenvironment near the transporter, which may alter homeostasis of DA neurons. Together, these changes would alter multiple properties of DA terminals. The functional consequences of these biophysical changes to *in vivo* physiology and pathology are yet to be discovered.

REFERENCES

1. Abramov, E., Dolev, I., Fogel, H., Ciccotosto, G. D., Ruff, E., and Slutsky, I. (2009) *Nat. Neurosci.* **12,** 1567–1576
2. Gray, B. C., Siskova, Z., Perry, V. H., and O'Connor, V. (2009) *Neurobiol. Dis.* **35,** 63–74
3. Zhang, C., Wu, B., Beglopoulos, V., Wines-Samuelson, M., Zhang, D., Dragatsis, I., Südhof, T. C., and Shen, J. (2009) *Nature* **460,** 632–636
4. Nemani, V. M., Lu, W., Berge, V., Nakamura, K., Onoa, B., Lee, M. K., Chaudhry, F. A., Nicoll, R. A., and Edwards, R. H. (2010) *Neuron* **65,** 66–79
5. Chandra, S., Fornai, F., Kwon, H. B., Yazdani, U., Atasoy, D., Liu, X., Hammer, R. E., Battaglia, G., German, D. C., Castillo, P. E., and Südhof, T. C. (2004) *Proc. Natl. Acad. Sci. U.S.A.* **101,** 14966–14971
6. Fujiwara, H., Hasegawa, M., Dohmae, N., Kawashima, A., Masliah, E., Goldberg, M. S., Shen, J., Takio, K., and Iwatsubo, T. (2002) *Nat. Cell Biol.* **4,** 160–164
7. Iwai, A., Masliah, E., Yoshimoto, M., Ge, N., Flanagan, L., de Silva, H. A., Kittel, A., and Saitoh, T. (1995) *Neuron* **14,** 467–475
8. Pronin, A. N., Morris, A. J., Surguchov, A., and Benovic, J. L. (2000) *J. Biol. Chem.* **275,** 26515–26522
9. Klivenyi, P., Siwek, D., Gardian, G., Yang, L., Starkov, A., Cleren, C., Ferrante, R. J., Kowall, N. W., Abeliovich, A., and Beal, M. F. (2006) *Neurobiol. Dis.* **21,** 541–548
10. Volkow, N. D., and Wise, R. A. (2005) *Nat. Neurosci.* **8,** 555–560
11. Reynolds, G. P. (1983) *Nature* **305,** 527–529
12. Iversen, L. (1992) *Nature* **358,** 109
13. Giros, B., Jaber, M., Jones, S. R., Wightman, R. M., and Caron, M. G. (1996) *Nature* **379,** 606–612
14. Rocha, B. A., Fumagalli, F., Gainetdinov, R. R., Jones, S. R., Ator, R., Giros, B., Miller, G. W., and Caron, M. G. (1998) *Nat. Neurosci.* **1,** 132–137
15. Amara, S. G., and Arriza, J. L. (1993) *Curr. Opin. Neurobiol.* **3,** 337–344
16. Amara, S. G., and Kuhar, M. J. (1993) *Annu. Rev. Neurosci.* **16,** 73–93
17. Torres, G. E. (2006) *J. Neurochem.* **97,** 3–10
18. Carneiro, A. M., Ingram, S. L., Beaulieu, J. M., Sweeney, A., Amara, S. G., Thomas, S. M., Caron, M. G., and Torres, G. E. (2002) *J. Neurosci.* **22,** 7045–7054
19. Lee, F. J., Liu, F., Pristupa, Z. B., and Niznik, H. B. (2001) *FASEB J.* **15,** 916–926
20. Lee, K. H., Kim, M. Y., Kim, D. H., and Lee, Y. S. (2004) *Neurochem. Res.* **29,** 1405–1409
21. Fog, J. U., Khoshbouei, H., Holy, M., Owens, W. A., Vaegter, C. B., Sen, N., Nikandrova, Y., Bowton, E., McMahon, D. G., Colbran, R. J., Daws, L. C., Sitte, H. H., Javitch, J. A., Galli, A., and Gether, U. (2006) *Neuron* **51,** 417–429
22. Gorentla, B. K., Moritz, A. E., Foster, J. D., and Vaughan, R. A. (2009) *Biochemistry* **48,** 1067–1076
23. Polymeropoulos, M. H., Lavedan, C., Leroy, E., Ide, S. E., Dehejia, A., Dutra, A., Pike, B., Root, H., Rubenstein, J., Boyer, R., Stenroos, E. S., Chandrasekharappa, S., Athanassiadou, A., Papapetropoulos, T., Johnson, W. G., Lazzarini, A. M., Duvoisin, R. C., Di Iorio, G., Golbe, L. I., and Nussbaum, R. L. (1997) *Science* **276,** 2045–2047
24. Zarranz, J. (2004) *Rev. Neurol.* **39,** 576–582

25. Zarranz, J. J., Alegre, J., Gómez-Esteban, J. C., Lezcano, E., Ros, R., Ampuero, I., Vidal, L., Hoenicka, J., Rodriguez, O., Atarés, B., Llorens, V., Gomez Tortosa, E., del Ser, T., Muñoz, D. G., and de Yebenes, J. G. (2004) *Ann. Neurol* **55,** 164–173

26. Singleton, A. B., Farrer, M., Johnson, J., Singleton, A., Hague, S., Kachergus, J., Hulihan, M., Peuralinna, T., Dutra, A., Nussbaum, R., Lincoln, S., Crawley, A., Hanson, M., Maraganore, D., Adler, C., Cookson, M. R., Muenter, M., Baptista, M., Miller, D., Blancato, J., Hardy, J., and Gwinn-Hardy, K. (2003) *Science* **302,** 841

27. Wersinger, C., Prou, D., Vernier, P., and Sidhu, A. (2003) *FASEB J.* **17,** 2151–2153

28. Wersinger, C., and Sidhu, A. (2003) *Neurosci. Lett.* **340,** 189–192

29. Gwinn-Hardy, K., Mehta, N. D., Farrer, M., Maraganore, D., Muenter, M., Yen, S. H., Hardy, J., and Dickson, D. W. (2000) *Acta Neuropathol.* **99,** 663–672

30. Mash, D. C., Ouyang, Q., Pablo, J., Basile, M., Izenwasser, S., Lieberman, A., and Perrin, R. J. (2003) *J. Neurosci.* **23,** 2564–2571

31. Farrer, M., Kachergus, J., Forno, L., Lincoln, S., Wang, D. S., Hulihan, M., Maraganore, D., Gwinn-Hardy, K., Wszolek, Z., Dickson, D., and Langston, J. W. (2004) *Ann. Neurol.* **55,** 174–179

32. Miller, D. W., Hague, S. M., Clarimon, J., Baptista, M., Gwinn-Hardy, K., Cookson, M. R., and Singleton, A. B. (2004) *Neurology* **62,** 1835–1838

33. Tong, J., Wong, H., Guttman, M., Ang, L. C., Forno, L. S., Shimadzu, M., Rajput, A. H., Muenter, M. D., Kish, S. J., Hornykiewicz, O., and Furukawa, Y. (2010) *Brain* **133,** 172–188

34. Larsen, K. E., Schmitz, Y., Troyer, M. D., Mosharov, E., Dietrich, P., Quazi, A. Z., Savalle, M., Nemani, V., Chaudhry, F. A., Edwards, R. H., Stefanis, L., and Sulzer, D. (2006) *J. Neurosci.* **26,** 11915–11922

35. Feng, L. R., Federoff, H. J., Vicini, S., and Maguire-Zeiss, K. A. (2010) *Eur. J. Neurosci.* **32,** 10–17

36. Zhang, D. Q., Stone, J. F., Zhou, T., Ohta, H., and McMahon, D. G. (2004) *Neuroreport.* **15,** 1761–1765

37. Kahlig, K. M., Binda, F., Khoshbouei, H., Blakely, R. D., McMahon, D. G., Javitch, J. A., and Galli, A. (2005) *Proc. Natl. Acad. Sci. U.S.A.* **102,** 3495–3500

38. Prasad, K. N., Clarkson, E. D., La Rosa, F. G., Edwards-Prasad, J., and Freed, C. R. (1998) *Mol. Genet. Metab.* **65,** 1–9

39. Sorkina, T., Doolen, S., Galperin, E., Zahniser, N. R., and Sorkin, A. (2003) *J. Biol. Chem.* **278,** 28274–28283

40. Clarkson, E. D., Edwards-Prasad, J., Freed, C. R., and Prasad, K. N. (1999) *Proc. Soc. Exp. Biol. Med.* **222,** 157–163

41. Zhou, W., Hurlbert, M. S., Schaack, J., Prasad, K. N., and Freed, C. R. (2000) *Brain Res.* **866,** 33–43

42. Miranda, M., Sorkina, T., Grammatopoulos, T. N., Zawada, W. M., and Sorkin, A. (2004) *J. Biol. Chem.* **279,** 30760–30770

43. Felix, K., Manna, S. K., Wise, K., Barr, J., and Ramesh, G. T. (2005) *J. Biochem. Mol. Toxicol.* **19,** 67–77

44. Mazzanti, M., and DeFelice, L. J. (1987) *Biophys. J.* **52,** 95–100

45. Mazzanti, M., and DeFelice, L. J. (1987) *Biophys. J.* **51,** 115–121

46. Goodwin, J. S., Larson, G. A., Swant, J., Sen, N., Javitch, J. A., Zahniser, N. R., De Felice, L. J., and Khoshbouei, H. (2009) *J. Biol. Chem.* **284,** 2978–2989

47. Khoshbouei, H., Sen, N., Guptaroy, B., Johnson, L., Lund, D., Gnegy, M. E., Galli, A., and Javitch, J. A. (2004) *PLoS Biol.* **2,** E78

48. Khoshbouei, H., Wang, H., Lechleiter, J. D., Javitch, J. A., and Galli, A.

49. Blakely, R. D., and DeFelice, L. J. (2007) *Mol. Pharmacol.* **71,** 1206–1208

50. Mason, J. N., Farmer, H., Tomlinson, I. D., Schwartz, J. W., Savchenko, V., DeFelice, L. J., Rosenthal, S. J., and Blakely, R. D. (2005) *J. Neurosci. Methods* **143,** 3–25

51. Schwartz, J. W., Novarino, G., Piston, D. W., and DeFelice, L. J. (2005) *J. Biol. Chem.* **280,** 19177–19184

52. Zapata, A., Kivell, B., Han, Y., Javitch, J. A., Bolan, E. A., Kuraguntla, D., Jaligam, V., Oz, M., Jayanthi, L. D., Samuvel, D. J., Ramamoorthy, S., and Shippenberg, T. S. (2007) *J. Biol. Chem.* **282,** 35842–35854

53. Bolan, E. A., Kivell, B., Jaligam, V., Oz, M., Jayanthi, L. D., Han, Y., Sen, N., Urizar, E., Gomes, I., Devi, L. A., Ramamoorthy, S., Javitch, J. A., Zapata, A., and Shippenberg, T. S. (2007) *Mol. Pharmacol.* **71,** 1222–1232

54. Lute, B. J., Khoshbouei, H., Saunders, C., Sen, N., Lin, R. Z., Javitch, J. A., and Galli, A. (2008) *Biochem. Biophys. Res. Commun.* **372,** 656–661

55. Oz, M., Jaligam, V., Galadari, S., Petroianu, G., Shuba, Y. M., and Shippenberg, T. S. (2010) *J. Neurochem.* **112,** 1454–1464

56. Schwartz, J. W., Blakely, R. D., and DeFelice, L. J. (2003) *J. Biol. Chem.* **278,** 9768–9777

57. Schwartz, J. W., Piston, D., and DeFelice, L. J. (2006) *Handb. Exp. Pharmacol.* **175,** 23–57

58. Carvelli, L., Blakely, R. D., and DeFelice, L. J. (2008) *Proc. Natl. Acad. Sci. U.S.A.* **105,** 14192–14197

59. Carvelli, L., McDonald, P. W., Blakely, R. D., and Defelice, L. J. (2004) *Proc. Natl. Acad. Sci. U.S.A.* **101,** 16046–16051

60. Gnegy, M. E., Khoshbouei, H., Berg, K. A., Javitch, J. A., Clarke, W. P., Zhang, M., and Galli, A. (2004) *Mol. Pharmacol.* **66,** 137–143

61. Ingram, S. L., and Amara, S. G. (2000) *J. Neurosci.* **20,** 550–557

62. Ingram, S. L., Prasad, B. M., and Amara, S. G. (2002) *Nat. Neurosci.* **5,** 971–978

63. Sonders, M. S., Zhu, S. J., Zahniser, N. R., Kavanaugh, M. P., and Amara, S. G. (1997) *J. Neurosci.* **17,** 960–974

64. Adams, F. S., La Rosa, F. G., Kumar, S., Edwards-Prasad, J., Kentroti, S., Vernadakis, A., Freed, C. R., and Prasad, K. N. (1996) *Neurochem. Res.* **21,** 619–627

65. Krueger, B. K. (1990) *J. Neurochem.* **55,** 260–267

66. Hong, W. C., and Amara, S. G. (2010) *J. Biol. Chem.* **285,** 32616–32626

67. van Rooijen, B. D., Claessens, M. M., and Subramaniam, V. (2010) *PLoS One* **5,** e14292

68. Zakharov, S. D., Hulleman, J. D., Dutseva, E. A., Antonenko, Y. N., Rochet, J. C., and Cramer, W. A. (2007) *Biochemistry* **46,** 14369–14379

69. Chandra, S., Gallardo, G., Fernández-Chacón, R., Schlüter, O. M., and Südhof, T. C. (2005) *Cell* **123,** 383–396

70. Cooper, A. A., Gitler, A. D., Cashikar, A., Haynes, C. M., Hill, K. J., Bhullar, B., Liu, K., Xu, K., Strathearn, K. E., Liu, F., Cao, S., Caldwell, K. A., Caldwell, G. A., Marsischky, G., Kolodner, R. D., Labaer, J., Rochet, J. C., Bonini, N. M., and Lindquist, S. (2006) *Science* **313,** 324–328

71. Gitler, A. D., Bevis, B. J., Shorter, J., Strathearn, K. E., Hamamichi, S., Su, L. J., Caldwell, K. A., Caldwell, G. A., Rochet, J. C., McCaffery, J. M., Barlowe, C., and Lindquist, S. (2008) *Proc. Natl. Acad. Sci. U.S.A.* **105,** 145–150

72. Lam, H. A., Wu, N., Cely, I., Kelly, R. L., Hean, S., Richter, F., Magen, I., Cepeda, C., Ackerson, L. C., Walwyn, W., Masliah, E., Chesselet, M. F., Levine, M. S., and Maidment, N. T. (2011) *J. Neurosci. Res.* **89,** 1091–1102

(2003) *J. Biol. Chem.* **278,** 12070–12077